
Article:
Liu, Bo, Liu, Shanshan, Yang, Long et al. (9 more authors) (2020) Light-Tunable Ferromagnetism in Atomically Thin Fe3GeTe2 Driven by Femtosecond Laser Pulse. Physical Review Letters. 267205. pp. 26-31. ISSN 1079-7114

https://doi.org/10.1103/PhysRevLett.125.267205

Light-tunable ferromagnetism in atomically-thin Fe_3GeTe_2 driven by femtosecond laser pulse

Bo Liu[1], Shanshan Liu[2], Long Yang[1], Zhendong Chen[1], Enze Zhang[2], Zihan Li[2], Jing Wu[3], Xuezhong Ruan[1*], Faxian Xiu[2,4*], Wenqing Liu[1,5], Liang He[1], Rong Zhang[1] and Yongbing Xu[1,3*]

[1] National Laboratory of Solid State Microstructures and Jiangsu Provincial Key Laboratory of Advanced Photonic and Electronic Materials, School of Electronic Science and Engineering, Nanjing University, Nanjing 210093, P. R. China

[2]State Key Laboratory of Surface Physics and Department of Physics, Fudan University, Shanghai 200433, P. R. China

[3]York-Nanjing Joint Center in Spintronics, Department of Electronic Engineering and Department of Physics, The University of York, York YO10 5DD, UK

[4]Institute for Nanoelectronic Devices and Quantum Computing, Fudan University, Shanghai 200433, P. R. China

[5] Department of Electronic Engineering, Royal Holloway University of London, Egham, Surrey TW20 0EX, UK

*Correspondence Emails: ybxu@nju.edu.cn, xzruan@nju.edu.cn and Faxian@fudan.edu.cn

Recent discovery of intrinsic ferromagnetism in two-dimension (2D) van der Waals (vdW) crystals has opened up a new arena for spintronics, raising an opportunity of achieving the tunable intrinsic 2D vdW magnetism. Here, we show that the magnetization and the magnetic anisotropy energy (MAE) of the few-layered Fe_3GeTe_2 (FGT) is strongly modulated by a femtosecond (fs) laser pulse. Upon increasing the fs laser excitation intensity, the saturation magnetization increases in an approximately linear way and the coercivity determined by the MAE, decreases monotonically, showing unambiguously the effect of the laser pulse on magnetic ordering. This effect observed at room temperature reveals the emergence of the light-driven room-temperature (300K) ferromagnetism in the 2D vdW FGT as its intrinsic Curie temperature T_C is ~ 200 K. The light-tunable ferromagnetism is attributed to the changes in the electronic structure due to the optical doping effect. Our findings pave a novel way to optically tune the 2D vdW magnetism and enhance the T_C up to the room temperature, promoting spintronic applications at or above the room temperature.

Magnetism in two-dimensional (2D) materials has been extensively studied both theoretically and experimentally due to the intriguing physics and the potential spintronic applications in magnetic data storage [1] and quantum information technologies [2,3]. Compared with bulk magnets, the 2D magnets have a distinctive advantage of building up various heterostructures with engineered levels of strain, chemistry, optical and electrical properties [4-7]. However, the extrinsically induced magnetic moments by chemical dopants [5], defects [6] or proximity layers [7] are usually low. Recently, the intrinsic ferromagnetism in 2D van der Waals (vdW) crystals, e.g. $Cr_2Ge_2Te_6$ [8], CrI_3 [9], VSe_2 [10] and $MnSe_2$ [11], has been experimentally observed, opening up a new arena for spintronic applications based on the vdW magnets, as well as for understanding the underlying physics. Unlike the ferromagnetism in conventional ultrathin films that is dependent on the interface quality and substrate properties, the 2D vdW magnets are less affected by these two factors as they do not require lattice matching. According to Mermin-Wagner theorem [12], the isotropic exchange interaction alone cannot sustain the long-range magnetic order in 2D limit at finite temperatures because of thermal fluctuations of the gapless spin-wave excitation energy. The observed intrinsic 2D ferromagnetism suggested that the presence of magnetic anisotropy energy (MAE) could give rise a spin-wave excitation gap and therefore maintain the long-range ferromagnetic order at finite temperatures [8]. Harnessing the intrinsic ferromagnetism in 2D vdW crystals thus requires a thorough knowledge of the exchange interaction and MAE. As a consequence, a fundamental question arises naturally: How can we tune the 2D ferromagnetism by modulating the exchange interaction and MAE via tailoring the electronic structures.

So far, the control and manipulation of the intrinsic magnetism are realized by couplings to external perturbations, including strain [13], gating [14-17], doping [18,19], and microstructure patterns [20]. For example, in semiconducting CrI_3 [17] and metallic Fe_3GeTe_2 [14], gating control causes changes in the magnetic properties such as the saturation magnetization, the coercivity and the transition temperature by indirectly tuning the exchange interactions and the density of states via the accumulated charge carriers. The manipulations of the intrinsic ferromagnetism in 2D vdW materials are mostly at low temperatures [15-17,21-25]. Recent reports on 2D ferromagnetism at or above room-temperature [10,11,14,19] push the vdW magnet based devices further towards practical applications. Despite these recent developments, the possibility of light-tuned magnetic properties in the intrinsic 2D vdW magnets is not established yet. With the optical approach, the magnetic properties can be continuously tailored and spatially addressed [26-28], which is proven to be feasible in layered vdW materials without intrinsic magnetism due to the strong light-matter interactions [29-31] as well as in ultrathin magnetic films [32,33] by modifying the exchange interactions or the MAE. Here, we explore for the first time the light control of the intrinsic ferromagnetism in vdW magnets. We choose the Fe_3GeTe_2 (FGT) as a candidate because the vdW FGT crystal has relatively high T_C (~220 K for bulk) and metallic character for spin source [22,34]. We show that a femtosecond (fs) pulsed laser efficiently tunes the magnetic ordering in atomically thin FGT films and surprisingly leads to the emergence of ferromagnetic order at room temperature. Upon fs laser excitations, both the saturation magnetization and the coercivity change with the laser intensity. The tunable magnetic properties, e.g., the exchange interaction, the T_C and the MAE, are attributed to the electronic structure changes. Specifically, under fs

excitations the excited photoholes below the Fermi level E_F shift the E_F downwards, crossing the enhanced DOS as indicated by the schematic diagram in Fig. 1(d). This leads to the Stoner instability and then strengthen the ferromagnetic order. This work provides an optical way to control the ferromagnetism in atomically thin FGT especially at room temperature.

Fig. 1(a) shows the atomic structure of FGT monolayer in side view (left) and the unit cell of FGT bi-layer (right). The lattice parameters of the unit cell are a = b ≈ 4 Å and c ≈ 16 Å [35]. Three Fe atoms in the unit cell are located in two inequivalent sites, referred to as Fe1 and Fe2, respectively. Each monolayer FGT consists of five sublayers (in top view), where the top and bottom layers are occupied by two Te atoms. The second and fourth layers are occupied by two Fe1 atoms and the middle layer is occupied by Ge and Fe2 atoms. The strong magneto-crystalline anisotropy along c-axis in FGT originates from the strong spin-orbital coupling (SOC) in Fe atoms [34]. The wafer-scale FGT thin films (~1 cm scale) are grown by molecular-beam epitaxy (MBE). The high-crystalline quality and the smooth surface are verified by the X-ray diffraction (XRD) and the streaky reflection high-energy electron diffraction (RHEED) patterns. Further growth conditions and the quality characterizations can be seen in the publications of our co-authors [36,37]. The sample thicknesses are 2 layers, 4 layers and 7 layers, respectively, with the monolayer thickness being 0.8 nm [36]. According to Hall resistance measurements (R_{xy}) from 10 K to 250 K as shown in Fig. 1(b), the T_C of 7-layer thick (5.6 nm) FGT is ~ 200 K. The T_C of the other two samples (4 layers and 2 layers) are ~ 140 K and ~ 134 K, respectively, which are also far below room temperature. The decreasing trend of T_C with decreasing sample thickness is consistent with the previous reports [38,39].

The magnetism of the high-quality FGT thin films is mainly studied by the static MOKE technique. In the measurements, we employed a fs pulsed laser with a repetition rate of 1 kHz, a pulse duration of ~50 fs and a central wavelength of 800 nm. As sketched in Fig. 1(c), The FGT magnetism is probed in the polar MOKE configuration using the 3.1 eV photon energy since the FGT has the out-of-plane magnetic anisotropy. The spot sizes of the laser beam on the sample surface is 200 μm in diameter. Note that here for static MOKE measurements we used a single beam of femtosecond laser pulses, which excites and probes the magnetism in FGT simultaneously. For comparison, we also used a continuous wave (cw) laser with a spot size of ~ 140 μm in diameter in static MOKE measurements (see supplemental material; c.f. Fig. S2).

In Fig. 2, under fs laser pulse excitations, the 7-, 4- and 2-layer FGT samples show clear magnetic hysteresis loops at the room temperature. By increasing the excitation intensity from 100 μw to 800 μw, the hysteresis loops of the three thin films are significantly modified by the fs laser pulse, with distinct variations of both Kerr rotations and coercivities. For clear display, the loops of 7-layer FGT at low fluences are multiplied by specific factors as indicated in Fig. 2(a). As the intrinsic T_c of the 7-layer FGT is ~ 200 K (see Fig. 1(b)), the obtained magnetic hysteresis loops at the room-temperature clearly demonstrate the emergence of the room-temperature ferromagnetism that can be tuned continuously by changing the intensity of

the fs laser pulses. In Fig. 2(b) and Fig. 2(c) the room-temperature ferromagnetism as well as its tunability is also clearly confirmed in 4-layer and 2-layer FGT samples.

To further reveal the evolutions of the light-tuned magnetic properties, we extract the saturated Kerr rotations and coercivities of the hysteresis loops of the FGT samples with different thicknesses. They are plotted in Fig. 3(a) and (b), respectively, as a function of the laser fluence. Here the saturated Kerr rotation represents the difference between the Kerr rotations measured at the positive and negative maximum external fields. In Fig. 3(a), the saturated Kerr rotations of 7-, 4- and 2-layer FGT increase linearly from ~ 22 to ~ 116 *mrad,* from ~ 9 to ~ 45 *mrad*, and from ~ 7 to ~ 20 *mrad*, respectively. The dash lines are guiding lines, exhibiting the approximately linear trend. The line slopes of thicker layers are larger. As shown in Fig. 3(b), the coercivity H_C drops gradually as the excitation fluence increases for all the three different layers FGT. Above the fluence of ~ 450 μw, H_C remains approximately unchanged, being ~ 5 Oe, 20 Oe and 25 Oe for 7 layers, 4 layers and 2 layers, respectively. It shows that the thinner FGT (e.g. 2 layers) has higher coercivities while the 7-layered sample has the lowest coercivity.

Generally, the easy axis coercivity H_c depends on several material parameters, including magnetic anisotropy, domain structure and magnetization reversal process (i.e. the coherent rotation) [38]. As shown in Fig. 1(b) and also in our previous work, the square hysteresis loops suggest the single (large) domain like behaviour with the out-of-plane MAE [36], which satisfies the Stoner model. Thus, the H_c in this study is proportional to the perpendicular magnetic anisotropy (PMA). Specifically, the H_c is expected to be ~ 0.5 H_K where H_K is the effective anisotropy field [40,41]. It has been demonstrated that the hole doping can suppress the coercivity and thus the PMA in FGT[18,34,42]. The MAE, an essential parameter to stabilize the ferromagnetic order in the vdW magnets, is primarily governed by the electronic states near the Fermi level [43]. Therefore, significant modifications of the magnetic properties are expected by tuning the material electronic structure with optical excitation.

The itinerant magnetic order in FGT was demonstrated previously to satisfy the Stoner criteria $ID(E_F) > 1$, where I is the Stoner parameter, describing the exchange energy between electrons with up- and down-spins, and $D(E_F)$ represents the density of states near the Fermi level [34,38]. As shown in Fig. 1(d) we display a simplified DOS diagram of the few-layered FGT films, which is derived from the calculated DOS of single layer FGT given by Zhuang *et al.* [34]. The schematic DOS is composed of 3d electrons (illustrated in green lines) that mainly provide the magnetic moments. After fs excitations by the 3-eV photon energy, majority (red) and minority electrons (grey) below the E_F are excited to the unoccupied states above the E_F, leaving excited holes near the E_F. The redistributed electronic states would shift the E_F down to the E_F' (as indicated by the black dash line), thus enhancing the DOS near the E_F'. As from our previous reports[36,37], the FGT samples are slightly hole-dominated. According to the Stoner theorem, the increased $D(E_F)$ will strengthen the ferromagnetic order of FGT films that corresponds to the enhancement of T_C. The increased saturation magnetization is the consequence of the enlarged difference between the majority and minority electron density. We also noticed that, in the monolayer $RuCl_3$, first-principles calculations showed that the engineered huge DOS within a narrow energy width by optically excited electron-hole pairs

could lead to a stable ferromagnetic phase [44]. In recent experiments the gate-tuned magnetism in the vdW magnets, e.g. Fe_3GeTe_2 [14] and $Cr_2Ge_2Te_6$ [15], is attributed to the rebalance of the spin-polarized electronic structures while tuning the Fermi level via electron or hole doping.

Via the optical excitations we observed significant decrease of the MAE, which consists of the uniaxial anisotropy (K_U) that originates from the spin-orbital interactions, favoring the out-of-plane magnetization, and the shape anisotropy (K_S) due to the dipolar interaction of magnetic moments, favoring the in-plane magnetization. Upon the shift of Fermi level, the band structure window dominated by the spin-orbital coupling also moves either close to or away from the Fermi level, corresponding to the increase and decrease of the K_U. In our case, the spin-orbital coupling induced bands should be pushed away from the Fermi level, leading to the decrease of K_U and thereby of the MAE. Analogous suppression of the MAE due to the E_F shift caused by the hole doping is reported in $Fe_{3-x}GeTe_2$ nanoflakes with detailed density function theory calculations and the angle-resolved photoelectron spectroscopy data [18].

The temperature influence is also taken into considerations as the ferromagnetic order is highly correlated with the temperature. The magnetic hysteresis loops of the three FGT samples indicate there are weak temperature dependences at a fixed laser fluence (c.f. Fig. S1). Compared to the light-intensity modulations, the saturated Kerr rotations and coercivities at different temperatures have similar values. A possible reason is that the spin ordering temperatures are enhanced greatly above room temperature by the fs pulsed laser and thus the light-tuned ferromagnetism exhibits little differences in the temperature range from 76 K to 300 K in this study. We have also found that the use of a fs laser pulse is necessary for tuning the ferromagnetism in atomically-thin FGT as verified by the MOKE measurements of the 7-layer FGT by using the cw laser. The wavelength of the cw laser is 405 nm, which is close to that of the fs pulsed laser. In Fig. S2, the hysteresis loop excited by the cw laser (red line) is negligible while the one caused by the fs pulsed-laser (black line) is clear. This may be due to the fact that within the 50-fs pulse duration the injected carrier density by the fs laser pulse is several orders of magnitude larger than that by the cw laser. Within the 50-fs period, the 100 μw fs pulses and the 2 mw cw laser excitation intensity corresponds to the fluences of 0.318 mJ/cm^2 and 0.26×10^{-12} mJ/cm^2, respectively. As the optical absorption coefficient of FGT is not available, the value of Fe [45] is used instead to estimate the injected carrier densities. The calculated injected carrier densities for the fs pulse laser and the cw laser are ~$3.2 \times 10^{14}/cm^2$ and ~ $3.3 \times 10^6/cm^2$, respectively. We found that the magnitude of the carrier density injected by the fs pulses is consistent with static electric gating[14].

Besides the qualitative analysis within the Stoner model, the magnetism of 2D vdW FGT can also be described by the anisotropic Heisenberg model [14] with the following effective Hamiltonian:

$$H = \sum_{i,j} J_{ij} \; S_i \cdot S_j + \sum_i A(S_i)^2 \qquad (1)$$

where S_i is the spin operator on the atom i, and J_{ij} is the exchange interaction between the neighboring spins on sites i and j; A represents the MAE which is perpendicular to the film plane. By applying the molecular-field approximation, the T_C is proportional to the $J_{ij} + A$. As a consequence, in our results to assure the enhancement of the T_C, the J_{ij} should increase under the optical fs excitations when the A (i.e. the MAE) decreases. Our ultrafast pump-probe measurements further reveal the temporal evolutions of the J_{ij}. Immediately after fs excitations, the transient hysteresis loops scale approximately linearly with the magnetic field, exhibiting the paramagnetic nature. Subsequently at large time-delays (~374 ps at 300 K), the transient hysteresis loops begin to show saturation property, indicating the appearance of the ferromagnetic phase and thus the enhancement of the J_{ij}. This ferromagnetic order can persist up to ~ 1.37 ns within our delay-line stage limit (see details in the Supporting Material). The enhanced T_C by modifying the exchange interaction J_{ij} is also observed in several vdW magnets, such as Fe_4GeTe_2 [46] and CrI_3 [13]. Overall our optical-tuned magnetism provides a unified understanding of the correlation between the modifications of magnetic properties and the electronic structure changes.

In conclusion, we demonstrate that a fs laser pulse can be exploited to tune the magnetism in the atomically thin vdW FGT magnets, achieving the continuously tunable saturation magnetization and the coercivity, and boosting the Curie temperature up to the room temperature. The significant modulations on the magnetic properties in FGT are related to the subtle changes in the electronic structure caused by the fs optical doping effect. In specific, the excited holes near the Fermi level leads to the redistribution of the electronic states, moving the Fermi level to the enhanced DOS. As a consequence, the ferromagnetic order (i.e., the Curie temperature and the exchange interaction) can be strengthened according to the Stoner criteria as well as the anisotropy Heisenberg model. The magnetic anisotropy is suppressed as the spin-orbit induced changes in the energy bands are pushed away from the Fermi level. Our findings demonstrate for the first time that the light-tunable magnetism has been achieved in the intrinsic 2D vdW FGT at room temperature, providing not only deeper understandings into the 2D ferromagnetism but also novel opportunities for exploiting the 2D vdW magnet for spintronic applications at room-temperature.

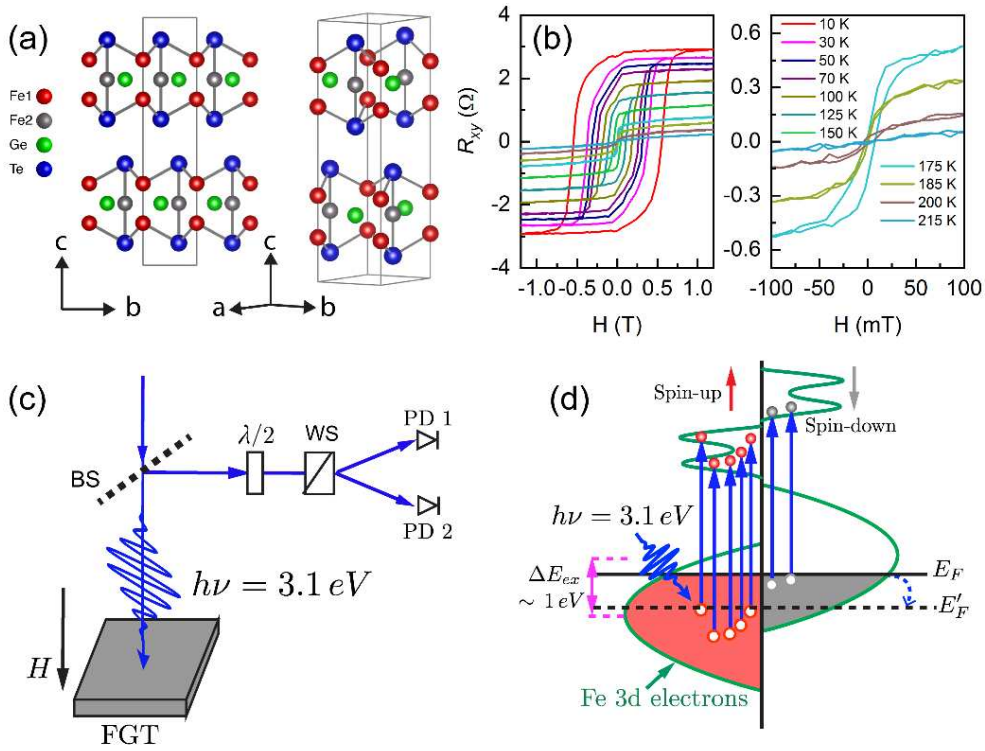

Fig. 1. Crystal structure of FGT and the characteristics of ferromagnetic transition temperature. (a) Side view (left) and unit cell (right) of FGT monolayer atomic structure. Fe1 and Fe2 represent two inequivalent sites of Fe atoms. (b) Temperature dependent Hall resistance (Rxy) of 7-layer thick vdW FGT as a function of perpendicular magnetic field. The left panel shows the Hall results from 10 K to 215 K while the right panel shows explicitly the results near T_C for clarity. (c) Diagram of experimental configuration for static MOKE measurements. Light-induced magnetism is measured via recording rotated polarization angles of the reflected single beam of femtosecond laser pulses. The BS and the WS here represent the beam splitter and Wollaston splitter, respectively. (d), Schematic of the laser-excited density of states (DOS) in few-layered FGT thin films. The photon energy of 3.1 eV, causes electron transitions (vertical blue arrows) from occupied states below the Fermi level E_F to the unoccupied states above the E_F. The simplified DOS diagram is derived from the calculated DOS of the single layer FGT in the reference [34] where the exchange splitting is estimated to be ~ 1 eV. See details in the main text.

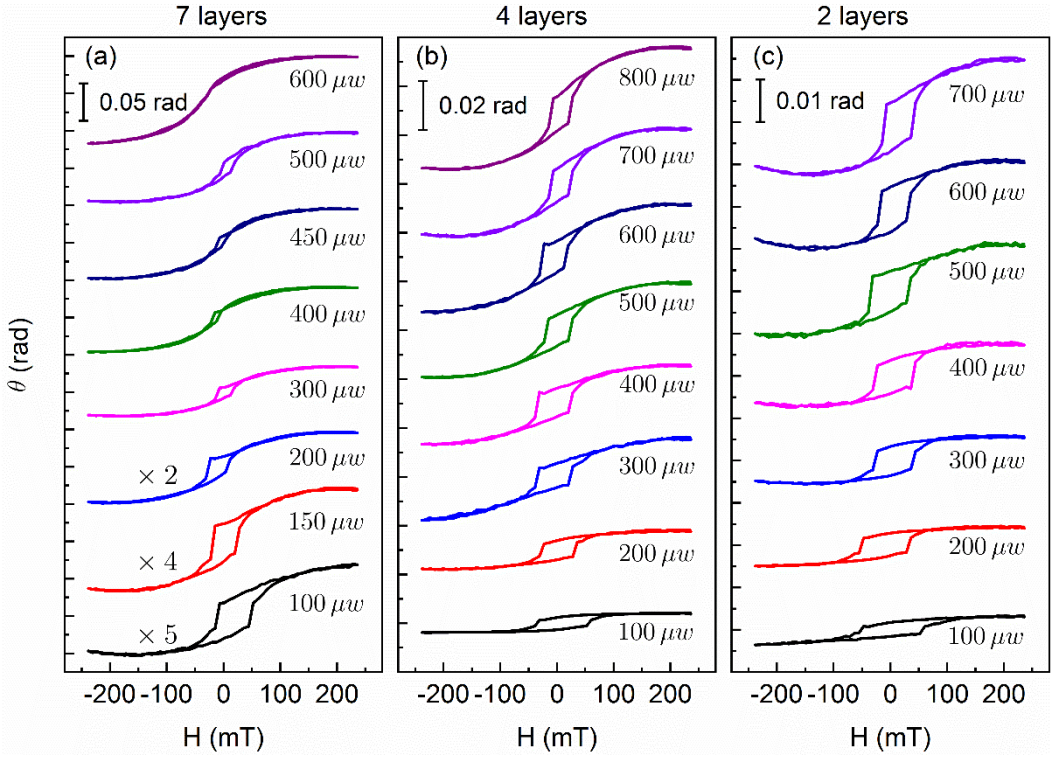

Fig. 2. Excitation fluence dependent ferromagnetism in atomically thin FGT films induced by the femtosecond pulsed laser in static MOKE measurements. (a) (b) and (c) show respectively the static magnetic hysteresis loops of 7-, 4- and 2-layer thickness at different excitation intensity of the pulsed laser at room temperature. The photon energy is 3.1 eV and obvious modifications on both Kerr rotations and coercivities are shown in all the thicknesses.

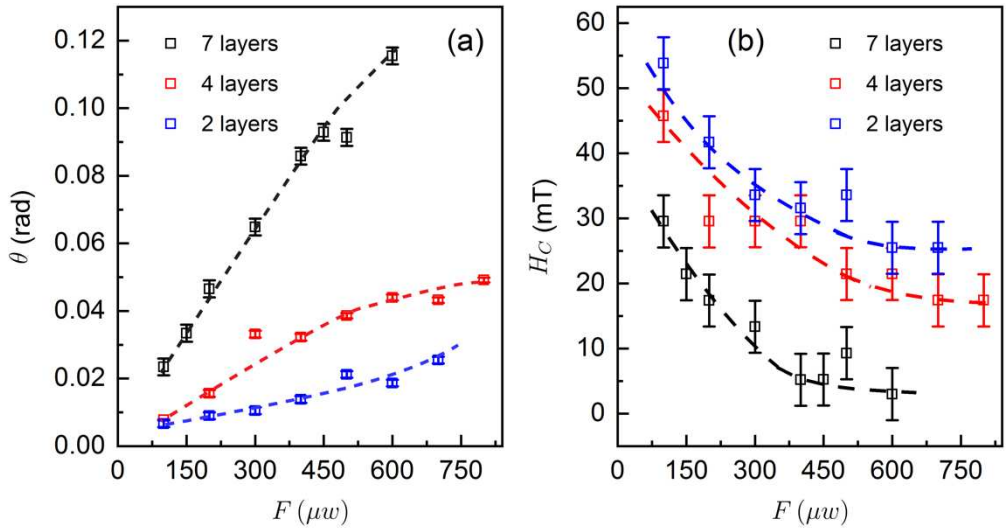

Fig. 3. (a) Extracted values of the saturated Kerr rotations and (b) coercivities of 7-, 4- and 2-layer FGT films as a function of the excitation fluence. The dash lines in (a) are guiding lines, showing the approximately linear response of the maximum Kerr rotations within the measured pump fluence range. The thicker layers of FGT show larger slopes of Kerr rotations but smaller coercivities. The dash guide lines in (b) exhibit the saturating trend of coercivities above the excitation fluence of 450 μw.

References

[1] A. Stupakiewicz, K. Szerenos, D. Afanasiev, A. Kirilyuk, and A. V. Kimel, Nature **542**, 71 (2017).

[2] D. D. Awschalom, R. Hanson, J. Wrachtrup, and B. B. Zhou, Nat. Photon. 1 (2018).

[3] T. Alexander and P. Natarajan, Science **345**, 1330 (2014).

[4] J.-G. Park, J. Phys.: Condens. Matter **28**, 301001 (2016).

[5] R. P. Jumde, F. Lanza, M. J. Veenstra, and S. R. Harutyunyan, Science **352**, 433 (2016).

[6] R. R. Nair, M. Sepioni, I.-L. Tsai, O. Lehtinen, J. Keinonen, A. V. Krasheninnikov, T. Thomson, A. K. Geim, and I. V. Grigorieva, Nat. Phys. **8**, 199 (2012).

[7] V. Lauter, F. S. Nogueira, B. A. Assaf, M. E. Jamer, P. Wei, B. Satpati, J. W. Freeland, I. Eremin, D. Heiman, P. Jarillo-Herrero, F. Katmis, and J. S. Moodera, Nature **533**, 513 (2016).

[8] C. Gong, L. Li, Z. Li, H. Ji, A. Stern, Y. Xia, T. Cao, W. Bao, C. Wang, Y. Wang, Z. Q. Qiu, R. J. Cava, S. G. Louie, J. Xia, and X. Zhang, Nature **546**, 265 (2017).

[9] B. Huang, G. Clark, E. Navarro-Moratalla, D. R. Klein, R. Cheng, K. L. Seyler, D. Zhong, E. Schmidgall, M. A. McGuire, D. H. Cobden, W. Yao, D. Xiao, P. Jarillo-Herrero, and X. Xu, Nature **546**, 270 (2017).

[10] M. Bonilla, S. Kolekar, Y. Ma, H. C. Diaz, V. Kalappattil, R. Das, T. Eggers, H. R. Gutierrez, M.-H. Phan, and M. Batzill, Nat. Nanotechnol. **13**, 289 (2018).

[11] D. J. O'Hara, T. Zhu, A. H. Trout, A. S. Ahmed, Y. K. Luo, C. H. Lee, M. R. Brenner, S. Rajan, J. A. Gupta, D. W. McComb, and R. K. Kawakami, Nano Lett. **18**, 3125 (2018).

[12] N. D. Mermin and H. Wagner, Phys. Rev. Lett. **17**, 1133 (1966).

[13] S. Chen, C. Huang, H. Sun, J. Ding, P. Jena, and E. Kan, J. Phys. Chem. C acs.jpcc.9b04631 (2019).

[14] Y. Deng, Y. Yu, Y. Song, J. Zhang, N. Z. Wang, Z. Sun, Y. Yi, Y. Z. Wu, S. Wu, J. Zhu, J. Wang, X. H. Chen, and Y. Zhang, Nature **563**, 94 (2018).

[15] Z. Wang, T. Zhang, M. Ding, B. Dong, Y. Li, M. Chen, X. Li, J. Huang, H. Wang, X. Zhao, Y. Li, Da Li, C. Jia, L. Sun, H. Guo, Y. Ye, D. Sun, Y. Chen, T. Yang, J. Zhang, S. Ono, Z. Han, and Z. Zhang, Nat. Nanotechnol. **13**, 554 (2018).

[16] S. Jiang, L. Li, Z. Wang, K. F. Mak, and J. Shan, Nat. Nanotechnol. **13**, 549 (2018).

[17] S. Jiang, J. Shan, and K. F. Mak, Nat. Mater. **17**, 406 (2018).

[18] S. Y. Park, D. S. Kim, Y. Liu, J. Hwang, Y. Kim, W. Kim, J.-Y. Kim, C. Petrovic, C. Hwang, S.-K. Mo, H.-J. Kim, B.-C. Min, H. C. Koo, J. Chang, C. Jang, J. W. Choi, and H. Ryu, Nano Lett. **20**, 95 (2020).

[19] F. Moro, M. A. Bhuiyan, Z. R. Kudrynskyi, R. Puttock, O. Kazakova, O. Makarovsky, M. W. Fay, C. Parmenter, Z. D. Kovalyuk, A. J. Fielding, M. Kern, J. van Slageren, and A. Patanè, Adv. Sci. **5**, 1800257 (2018).

[20] Q. Li, M. Yang, C. Gong, R. V. Chopdekar, A. T. N'Diaye, J. Turner, G. Chen, A. Scholl, P. Shafer, E. Arenholz, A. K. Schmid, S. Wang, K. Liu, N. Gao, A. S. Admasu, S.-W. Cheong, C. Hwang, J. Li, F. Wang, X. Zhang, and Z. Qiu, Nano Lett. **18**, 5974 (2018).

[21] M. Abramchuk, S. Jaszewski, K. R. Metz, G. B. Osterhoudt, Y. Wang, K. S. Burch, and F. Tafti, Adv. Mater. **30**, 1801325 (2018).
[22] Z. Wang, D. Sapkota, T. Taniguchi, K. Watanabe, D. Mandrus, and A. F. Morpurgo, Nano Lett. **18**, 4303 (2018).
[23] Z. Wang, I. Gutiérrez-Lezama, N. Ubrig, M. Kroner, M. Gibertini, T. Taniguchi, K. Watanabe, A. Imamoğlu, E. Giannini, and A. F. Morpurgo, Nat. Commun. **9**, 2516 (2018).
[24] A. M. Tokmachev, D. V. Averyanov, O. E. Parfenov, A. N. Taldenkov, I. A. Karateev, I. S. Sokolov, O. A. Kondratev, and V. G. Storchak, Nat. Commun. **9**, 1672 (2018).
[25] T. Song, X. Cai, M. W.-Y. Tu, X. Zhang, B. Huang, N. P. Wilson, K. L. Seyler, L. Zhu, T. Taniguchi, K. Watanabe, M. A. McGuire, D. H. Cobden, D. Xiao, W. Yao, and X. Xu, Science **360**, 1214 (2018).
[26] L. Yang, N. A. Sinitsyn, W. Chen, J. Yuan, J. Zhang, J. Lou, and S. A. Crooker, Nat. Phys. **11**, 830 (2015).
[27] X. Xu, W. Yao, D. Xiao, and T. F. Heinz, Nat. Phys. **10**, 343 (2014).
[28] A. M. Jones, H. Y. Yu, N. J. Ghimire, S. F. Wu, G. Aivazian, J. S. Ross, B. Zhao, J. Q. Yan, D. G. Mandrus, D. Xiao, W. Yao, and X. D. Xu, Nat. Nanotechnol. **8**, 634 (2013).
[29] L. Britnell, R. M. Ribeiro, A. Eckmann, R. Jalil, B. D. Belle, A. Mishchenko, Y. J. Kim, R. V. Gorbachev, T. Georgiou, S. V. Morozov, A. N. Grigorenko, A. K. Geim, C. Casiraghi, A. H. C. Neto, and K. S. Novoselov, Science **340**, 1311 (2013).
[30] M. Bernardi, M. Palummo, and J. C. Grossman, Nano Lett. **13**, 3664 (2013).
[31] V. O. Jimenez, Y. T. H. Pham, M. Liu, F. Zhang, V. Kalappattil, B. Muchharla, T. Eggers, D. L. Duong, M. Terrones, and M.-H. Phan, arXiv:2007.01505 (2020).
[32] P. Tengdin, C. Gentry, A. Blonsky, D. Zusin, M. Gerrity, L. Hellbrück, M. Hofherr, J. Shaw, Y. Kvashnin, E. K. Delczeg-Czirjak, M. Arora, H. Nembach, T. J. Silva, S. Mathias, M. Aeschlimann, H. C. Kapteyn, D. Thonig, K. Koumpouras, O. Eriksson, and M. M. Murnane, Sci. Adv. **6**, eaaz1100 (2020).
[33] E. Hendry, A. Secchi, J. H. Mentink, M. Eckstein, A. Wu, R. V. Pisarev, V. V. Kruglyak, M. I. Katsnelson, T. Rasing, A. V. Kimel, and R. V. Mikhaylovskiy, Nat. Commun. 1 (2019).
[34] H. L. Zhuang, P. R. C. Kent, and R. G. Hennig, Phys. Rev. B **93**, 134407 (2016).
[35] J.-X. Zhu, M. Janoschek, D. S. Chaves, J. C. Cezar, T. Durakiewicz, F. Ronning, Y. Sassa, M. Mansson, B. L. Scott, N. Wakeham, E. D. Bauer, and J. D. Thompson, Phys. Rev. B **93**, 14404 (2016).
[36] S. Liu, X. Yuan, Y. Zou, Y. Sheng, C. Huang, E. Zhang, J. Ling, Y. Liu, W. Wang, C. Zhang, J. Zou, K. Wang, and F. Xiu, Npj 2D Materials and Applications **1**, 1 (2017).
[37] S. Liu, K. Yang, W. Liu, E. Zhang, Z. Li, X. Zhang, Z. Liao, W. Zhang, J. Sun, Y. Yang, H. Gao, C. Huang, L. Ai, P. K. J. Wong, A. T. S. Wee, A. T. N'Diaye, S. A. Morton, X. Kou, J. Zou, Y. Xu, H. Wu, and F. Xiu, Natl. Sci. Rev. **7**, 745 (2019).
[38] C. Tan, J. Lee, S.-G. Jung, T. Park, S. Albarakati, J. Partridge, M. R. Field, D. G. McCulloch, L. Wang, and C. Lee, Nat. Commun. **9**, 1554 (2018).

[39] Z. Fei, B. Huang, P. Malinowski, W. Wang, T. Song, J. Sanchez, W. Yao, Di Xiao, X. Zhu, A. F. May, W. Wu, D. H. Cobden, J.-H. Chu, and X. Xu, Nat. Mater. **17**, 778 (2018).
[40] G. Long, H. Zhang, D. Li, R. Sabirianov, Z. Zhang, and H. Zeng, Appl. Phys. Lett. **99**, 202103 (2011).
[41] E. C. STONER and E. P. WOHLFARTH, Philosophical Transactions of the Royal Society of London Series a-Mathematical and Physical Sciences **240**, 599 (1948).
[42] A. F. May, S. Calder, C. Cantoni, H. Cao, and M. A. McGuire, Phys. Rev. B **93**, 014411 (2016).
[43] D.-S. Wang, R. Wu, and A. J. Freeman, Phys. Rev. B **47**, 14932 (1993).
[44] Y. Tian, W. Gao, E. A. Henriksen, J. R. Chelikowsky, and L. Yang, Nano Lett. **19**, 7673 (2019).
[45] P. B. Johnson and R. W. Christy, Phys. Rev. B **9**, 5056 (1974).
[46] J. Seo, D. Y. Kim, E. S. An, K. Kim, G.-Y. Kim, S.-Y. Hwang, D. W. Kim, B. G. Jang, H. Kim, G. Eom, S. Y. Seo, R. Stania, M. Muntwiler, J. Lee, K. Watanabe, T. Taniguchi, Y. J. Jo, J. Lee, B. I. Min, M. H. Jo, H. W. Yeom, S.-Y. Choi, J. H. Shim, and J. S. Kim, Sci. Adv. **6**, eaay8912 (2020).

Acknowledgments This work is supported by National Key Research and Development Program of China (Grant No. 2016YFA0300803, 2017YFA0303302, 2018YFA0305601), the National Natural Science Foundation of China (Grant No. 61427812, 11774160, 61674040, 11874116), the Science and Technology Commission of Shanghai (Grant No. 19511120500), the Natural Science Foundation of Jiangsu Province of China (No. BK20192006), the Fundamental Research Funds for the Central Universities (Grant No. 021014380113), National Science and Technology Major Project (2017ZX01032101-001), UK EPSRC (EP/S010246/1), Royal Society (IEC\NSFC\181680), and Leverhulme Trust (LTSRF1819\15\12).

Author Contributions: Y.X. and X.R. conceived and supervised the project. B.L. performed the experiments with the help of X.R., Z.C. and L.Y.. F.X., S.L., E.Z. and Z.L. prepared Fe_3GeTe_2 thin films and also characterized them via the transport measurements. B.L., X.R., J.W., F.X., and Y.X. contributed to the analysis of the experiment data. B.L wrote the paper with the input from all authors.

Competing interests: The authors declare no conflicts of interests.

Data available: All data files are available by requesting the corresponding author